

The Higgs Transverse Momentum Distribution at NNLL and its Theoretical Errors

Duff Neill,^a Ira Z. Rothstein^b Varun Vaidya^b

^b*Department of Physics, Carnegie Mellon University, Pittsburgh, PA 15213, U.S.A.*

^a*Center for Theoretical Physics, Massachusetts Institute of Technology, Cambridge MA 022139 U.S.A.*

ABSTRACT: In this letter, we present the NNLL-NNLO transverse momentum Higgs distribution arising from gluon fusion. In the regime $p_{\perp} \ll m_H$ we include the resummation of the large logs at next to next-to leading order and then match on to the α_s^2 fixed order result near $p_{\perp} \sim m_h$. By utilizing the rapidity renormalization group (RRG) we are able to smoothly match between the resummed, small p_{\perp} regime and the fixed order regime. We give a detailed discussion of the scale dependence of the result including an analysis of the rapidity scale dependence. Our central value differs from previous results, in the transition region as well as the tail, by an amount which is outside the error band. This difference is due to the fact that the RRG profile allows us to smoothly turn off the resummation.

Contents

1	Introduction	1
2	Systematics	2
3	Factorization in SCET and anomalous dimension	3
4	Renormalization and Resummation	5
5	The Fixed Order Cross Section and Power Corrections	7
6	Profiles	8
7	Error analysis	8
8	Comparison to Previous Results	12
9	Conclusion	16
10	Acknowledgements	16
A	RRG resummation	17
A.1	Comparison to Grazzini et al.	19

1 Introduction

We are transitioning into an era of precisions Higgs physics. Presently there is sufficient data to study various decay modes of the Higgs [1], and soon there will be sufficient data to study the the Higgs differential cross section, which can be used to better understand the underlying production mechanism and to search for new physics [2]. While the new physics would be most prominent at large values of p_\perp , the predominance of the events will be in the lower range. Furthermore, to isolate the Higgs' decays from backgrounds, events are binned according to their highest-transverse momentum jet. The 0-jet bin, corresponding to no central jets above a certain transverse-momentum threshold, plays a critical role in the current Higgs analysis ¹. Thus there is increased motivation for making precise predictions for the distribution when $p_\perp \ll m_h$ since back to back central jet production is power suppressed [15].

¹Resummed predictions for the 0-jet bin can be found in [4–8].

The small p_\perp region of parameter space is polluted by large logarithms which must be resummed in order to retain systematic control of the theoretical errors. Resummations have been previously been discussed within an SCET [3] framework [[17],[20],[21],[18],[22],[23],[25],[27],[26]] as well as in the CSS resummation formalism [[28],[29],[30],[31],[33],[32]]. While formally most of these results agree at a given order in the resummation procedure, the central values as well as the predicted errors between different resummation techniques will differ². Another crucial difference between various theoretical predictions is how the transition between the fixed order result at large p_\perp and the resummed result is handled. In this paper we present a result for the resummed cross section at NNLL + NNLO within the confines of SCET and the rapidity renormalization group (RRG) [14, 15]. Our motivation for this analysis is two-fold. By working within the RRG formalism we are able to consistently turn off the resummation in the tail region. It has been shown in the context of $B \rightarrow X_s + \gamma$ [48], thrust [49] as well as the Higgs jet veto calculation [44], that if one does not turn off the resummation then one can over estimate the cross section, in the region where fixed order perturbation theory should suffice, by an amount which goes beyond the canonical error band in the fixed order result. This overshoot happens despite the fact that the resummed terms are formally sub-leading in the expansion. The reason for this overshoot has been shown [44, 48, 49] to be due to the fact that there are cancellations between the singular and non-singular terms in the tail region and that this cancellation will occur only if the proper scale is chosen in the logarithms. This will be born out in our analysis as well. By using the RRG we have a natural way to interpolate between the resummed and fixed order regions. This allows us to present the full spectrum such that in the large p_\perp region our results match onto the NNLO result, as previously discussed within the context of the jet veto cross section [7, 8]. In this sense our paper fills a gap in the literature. As we will discuss below, the RRG plays an important role in the theory error determination. We also discuss in detail how our error estimates and full spectrum differ from those of previous work.

2 Systematics

In this section, for the sake of completeness, we review the well known systematics of the calculation. We work within the confines of the large top mass approximation. This approximation is known to work extremely well - much better than one would naively expect - especially away from the tail of the spectrum. We will not be considering p_\perp large enough for these corrections to be relevant to the error budget. A full discussion of such errors as well as others will be discussed at the end of the paper.

At the scale m_t , full QCD is matched onto the large top mass effective theory at order α_s^2 , after which we match onto SCET at the scale m_h . In SCET we will work to leading order in a systematic expansion in p_\perp/m_h , and the errors due to non-perturbative corrections, which are suppressed by Λ/p_\perp , are included in the final error analysis.

²For a detailed comparison of resummation methods in the context of e^+e^- event shapes see [57], and for threshold resummations see [34, 35].

As is well known, logs in the perturbative expansion - in impact parameter space - exponentiate and allow us to organize the series as follows

$$\sigma \sim \text{Exp} \left[\ln(bm_h) F(\alpha_s \ln(bm_h)) + G(\alpha_s \ln(bm_h)) + \alpha_s H(\alpha_s \ln(bm_h)) + \dots \right]. \quad (2.1)$$

The standard terminology is such that keeping only F corresponds to “LL” leading (double) log, while if G is retained we would have NLL etc. As p_\perp gets larger the EFT breaks down and the fixed order calculation becomes the relevant quantity. We will utilize the order α^2 (NNLO) result [9], [10]³ in this large p_\perp region. We do so despite the fact in the small p_\perp region we will be only keeping terms of order α . This is not inconsistent as the error in the two disparate regions are distinct and uncorrelated. In the resummed region we will be working at NNLL in the perturbative expansion and at leading order in the power expansion p_\perp/m_h . By utilizing the RRG scale we will smoothly turn off the resummation and match onto the full NNLO fixed order calculation.

3 Factorization in SCET and anomalous dimension

A factorization theorem for Higgs production at small p_\perp within SCET and the RRG formalism was developed in [15]. The starting point in the large top mass effective theory is the gluon fusion operator

$$\mathcal{H}(x) = C_t \frac{h(x)}{v} \text{Tr}[G^{\mu\nu}(x)G_{\mu\nu}(x)]. \quad (3.1)$$

The matching coefficient for this operator (C_t) is known to two loops [12].

At the scale m_h ⁴ we match onto SCETII. This theory is the version of SCET in which the collinear modes and the soft modes have the same invariant mass, which distinguishes it from SCETI where there exists a hierarchy in masses between these two modes. Due to this equality in virtualities a new set of divergences - rapidity divergences - arise, which are not regulated by dimensional regularization. The rapidity regulator introduces a new scale which acts as a boundary between the collinear and soft modes as discussed in [14, 15]. The reader may consult ([15]) for the details of the formalism. At leading order in $\lambda = p_\perp/M_h$ the differential cross section for higgs production at low transverse momentum may be written as

$$\begin{aligned} \frac{d\sigma}{dp_\perp^2 dy} &= \frac{C_t^2}{8v^2 S(N_c^2 - 1)} \int \frac{d^4 p_h}{(2\pi)^4} (2\pi) \delta^+(p_h^2 - m_h^2) \delta\left(y - \frac{1}{2} \ln \frac{p_h^+}{p_h^-}\right) \delta(p_\perp^2 - |\vec{p}_{h\perp}|^2) \\ &\quad 4(2\pi)^8 \int d^4 x e^{-ix \cdot p_h} H(m_h) f_{\perp g/P}^{\mu\nu}(0, x^+, \vec{x}_\perp) f_{\perp g/P \mu\nu}(x^-, 0, \vec{x}_\perp) \mathcal{S}(0, 0, \vec{x}_\perp) \end{aligned} \quad (3.2)$$

³As is common with fixed order calculations, the authors of [10] use the term NLO, since the leading order result is a delta function in p_\perp .

⁴We ignore the running between the top mass scale and m_h as these logs will be sub-leading in our power counting.

\mathcal{S} is the soft function defined as

$$\mathcal{S}(0, 0, \vec{x}_\perp) = \frac{1}{(2\pi)^2(N_c^2 - 1)} \langle 0 | S_n^{ac}(x) S_{\bar{n}}^{ad}(x) S_n^{bc}(0) S_{\bar{n}}^{bd}(0) | 0 \rangle, \quad (3.3)$$

defined in terms of the light-like Wilson lines

$$S_n(x) = P \exp \left(ig \int_{-\infty}^0 n \cdot A_s(n\lambda + x) d\lambda \right). \quad (3.4)$$

$f^{\alpha\beta}$ is the transverse momentum distribution function (TMPDF) which is matched onto the PDFs at the scale $p_\perp \gg \Lambda$.

$$\begin{aligned} f_{\perp g/P}^{\mu\nu}(0, x^+, \vec{x}_\perp) &= \frac{1}{2(2\pi)^3} \langle p_n | [B_{n\perp}^{A\mu}(x^+, \vec{x}_\perp) B_{n\perp}^{A\nu}(0)] | p_n \rangle, \\ f_{\perp g/P}^{\mu\nu}(x^-, 0, \vec{x}_\perp) &= \frac{1}{2(2\pi)^3} \langle p_{\bar{n}} | [B_{\bar{n}\perp}^{A\mu}(x^-, \vec{x}_\perp) B_{\bar{n}\perp}^{A\nu}(0)] | p_{\bar{n}} \rangle \end{aligned} \quad (3.5)$$

defined in terms of

$$B_{n\perp}^{a\mu}(x) = \frac{2}{g} \text{Tr} \left[T^a \left[W_n^\dagger(x) i D_{n\perp}^\mu W_n(x) \right] \right]. \quad (3.6)$$

W_n is a collinear Wilson line in the fundamental representation defined in x -space by

$$W_n(x) = P \exp \left(ig \int_{-\infty}^x \bar{n} \cdot A_n(\bar{n}\lambda) d\lambda \right). \quad (3.7)$$

$n/\bar{n} = (1, 0, 0, \pm 1)$ are the null vectors which correspond to the directions of the incoming protons. In impact parameter space, we can write the functions S and $f^{\alpha\beta}$ in terms of their inverse Fourier transform.

$$S(b) = \int \frac{d^2 \vec{P}_{s\perp}}{(2\pi)^2} e^{i\vec{b} \cdot \vec{P}_{s\perp}} S(\vec{P}_{s\perp}) \quad (3.8)$$

$$f_n^{\mu\nu}(b, z) = \int \frac{d^2 \vec{P}_\perp}{(2\pi)^2} e^{i\vec{b} \cdot \vec{P}_\perp} f_n^{\mu\nu}(\vec{P}_\perp, z). \quad (3.9)$$

The cross section is given by

$$\frac{d^2 \sigma}{dP_t^2 dy} = \pi(2\pi)^5 \frac{H(M_h) \pi C_t^2}{2v^2 s^2 (N_c^2 - 1)} \int db b J_0(b P_t) f_n^{\alpha\beta}(b, z_1) f_{\alpha\beta, n'}(b, z_2) S(b) \quad (3.10)$$

$H(M_h)$ is the hard coefficient which depends on the scale $\mu = M_h$ and we define $H(M_h) = 8M_h^2 |C_s|^2$, where the coefficient C_s is known to two loops [13]. The soft function as well as the TMPDFs depend upon both μ , the usual scale introduced within the context of dimensional regularization which factorizes the hard modes from the soft and collinear modes, as well as ν , the rapidity factorization scale which distinguishes between the soft and collinear modes.

4 Renormalization and Resummation

Each of the pieces of the factorization theorem H , \mathcal{S} and f , have natural scales with which they are associated. H is independent of ν and its natural μ scale is m_h . The soft and collinear functions have natural scales $(\mu = p_\perp, \nu = p_\perp)$ and $(\mu = p_\perp, \nu = m_h)$ respectively. When these objects are evaluated at these scales, they will be devoid of large logarithms. However, given the natural distribution of scales we can see that it is not possible to choose a μ and ν such that all of the individual pieces sit at their respective natural scales. Thus it is expedient to choose a (μ, ν) value such that the maximum number of pieces sit at their natural scale, and then use the RG and RRG to sum logs for the remaining pieces.

The individual functions satisfy the following RGE's.

$$\mu \frac{d}{d\mu} H(\mu) = \gamma_\mu^H H(\mu)$$

$$\kappa_i \frac{d}{d\kappa_i} F(b, \mu, \nu) = \gamma_{\kappa_i}^F F(b, \mu, \nu) \quad (4.1)$$

$$(4.2)$$

where $\kappa_i = (\mu, \nu)$ and $F \in \{\mathcal{S}, f^{\alpha\beta}\}$. The anomalous dimensions satisfy the relations

$$\gamma_\mu^H + \gamma_\mu^S + 2\gamma_\mu^f = 0$$

$$\gamma_\nu^S + 2\gamma_\nu^f = 0. \quad (4.3)$$

All the renormalization group equations are diagonal in impact parameter space and hence are straightforward to solve. The scales for RG and RRG operations commute, and as a consequence of this, the following relations are generated

$$\mu \frac{d}{d\mu} \gamma_\nu^S = \nu \frac{d}{d\nu} \gamma_\mu^S = -2\Gamma_{cusp} \quad (4.4)$$

$$\mu \frac{d}{d\mu} \gamma_\nu^f = \nu \frac{d}{d\nu} \gamma_\mu^f = \Gamma_{cusp}, \quad (4.5)$$

where Γ_{cusp} is the cusp anomalous dimensions of two light-like Wilson lines [37].

Figure (1) shows the path in (μ, ν) space we have chosen to resum the logs. The hard part is run from the scales m_h down to the scale $1/b_0 \sim p_\perp$, while the jet function is run in ν space up to the scale m_h , where the scale b_0 is defined as $be^{\gamma_E}/2$. In performing the hard resummation, π^2 are resummed by analytically continuing the matching scale from space-like to time-like kinematics relevant for Higgs production[39]. It has been shown that the inclusion of the π^2 in the resummation does improve the perturbative convergence of the hard matching expansion [19, 40], however this method only sums a subset of π^2 and one can not claim that this method leads to a systematic reduction in theory errors ⁵.

At NNLL, the systematics require that we keep the cusp anomalous dimensions at three loops, the non-cusp at two loops and matching at both the high and low scales at order α . All

⁵There is no scaling rule for these terms

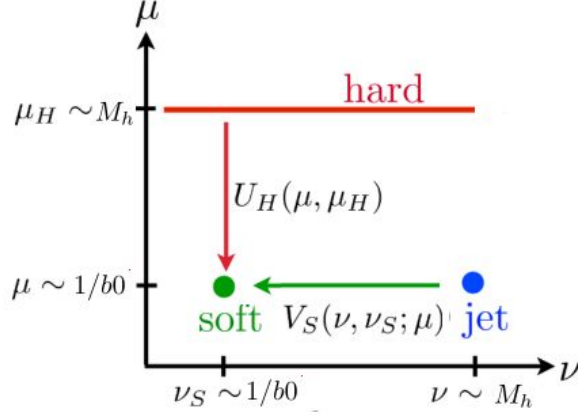


Figure 1. The path in (μ, ν) space used to resum the logs.

of the necessary anomalous dimensions have been calculated previously in the literature. The hard anomalous dimensions can be extracted from [43]. We utilize the one loop matching for the jet and soft function from ([15]). To run the jet function in ν we need only the two loop cusp piece since log in jet rapidity the anomalous dimension is not large. The coefficient of this log is fixed by the hard function anomalous dimensions. We also need the two loop “non-cusp” piece in ν which can be obtained from the two loop jet function. The results for the hard anomalous dimension are tabulated in [44].

The matching of the TMPDF onto the PDF may be written as

$$f_{\perp g/P}^{R\mu\nu}(z, \vec{p}_\perp) = \sum_k \frac{1}{z} \int_z^1 \frac{dz'}{z'} \left\{ \frac{g_\perp^{\mu\nu}}{2} I_{\perp 1 g/k}(z/z', \vec{p}_\perp^2) + \left(\frac{\vec{p}_\perp^\mu \vec{p}_\perp^\nu}{\vec{p}_\perp^2} + \frac{g_\perp^{\mu\nu}}{2} \right) I_{\perp 2 g/k}(z/z', \vec{p}_\perp^2) \right\} f_{k/P}^R(z') + O\left(\frac{\Lambda_{QCD}}{|\vec{p}_\perp|}\right), \quad (4.6)$$

where the sum is on species of partons, and the parton PDF’s are defined as

$$f_{g/P}(z) = -z \bar{n} \cdot p_n \theta(z) g_{\perp\mu\nu} \langle p_n | [B_{n\perp}^{c\mu}(0) \delta(z \bar{n} \cdot p_n - \bar{\mathcal{P}}) B_{n\perp}^{c\nu}(0)] | p_n \rangle. \\ f_{q/P}(z) = -z \bar{n} \cdot p_n \theta(z) \langle p_n | \left[\bar{\xi}_{n,p}^q(0) W_n \frac{\not{n}}{2} \delta(z \bar{n} \cdot p_n - \bar{\mathcal{P}}) W_n^\dagger \xi_{n,p}^q(0) \right] | p_n \rangle. \quad (4.7)$$

We adopt the mostly minus metric such that conventions that $\vec{p}_\perp^\alpha \vec{p}_\perp^\beta g_{\perp\alpha\beta} = -\vec{p}_\perp^2$ and make use of the ’t Hooft-Veltmann scheme, so the external transverse momenta remains in 2 dimensions, as do the external polarizations on the operator (the free Lorentz induces). The scheme choice is advantageous, as it allows one to renormalize the operator directly in \vec{p}_\perp space. At tree

level the TMDPDF matches on to the PDF as follows:

$$f_{\perp g/g}^{(0)\alpha\beta}(z, \vec{p}_\perp) = \delta(1-z)\delta^{(2)}(\vec{p}_\perp) \frac{g_\perp^{\alpha\beta}}{2} f_{g/P}(z). \quad (4.8)$$

$$(4.9)$$

The one loop renormalized TMDPDF, necessary to extract the order α matching coefficients ($I_{\perp ig/g}^{(1,2)}$), is given by

$$\begin{aligned} I_{\perp 1g/g}(z/z', \vec{p}_\perp^2) &= \frac{\alpha_s C_A}{\pi} \mathcal{L}_0\left(\mu, \frac{\vec{p}_\perp}{\mu}\right) \left(-\ln\left(\frac{\nu^2}{\omega_-^2}\right) \delta(1-z) + p_{gg^*}(z) \right) \\ I_{\perp 2g/g}(z/z', \vec{p}_\perp^2) &= -2 \frac{\alpha_s C_A}{\pi} \frac{1-z}{z} \mathcal{L}_0\left(\mu, \frac{\vec{p}_\perp}{\mu}\right) \left(\frac{\vec{p}_\perp^\alpha \vec{p}_\perp^\beta}{\vec{p}_\perp^2} + \frac{g_\perp^{\alpha\beta}}{2} \right) \\ I_{\perp 1g/q}(z/z', \vec{p}_\perp^2) &= \frac{\alpha_s C_F}{\pi} \left(\mathcal{L}_0\left(\mu, \frac{\vec{p}_\perp}{\mu}\right) P_{gq}(z) + \delta^{(2)}(\vec{p}_\perp) R_{gq}(z) \right) \end{aligned} \quad (4.10)$$

where we have written the expression in terms of plus distribution $\mathcal{L}_n = \frac{1}{2\pi\mu^2} \left[\frac{\mu^2}{\vec{p}_\perp^2} \ln^n \left(\frac{\mu^2}{\vec{p}_\perp^2} \right) \right]_+$, the properties of this distribution are collected in the appendix of [15].

The resummation is carried out in impact parameter space and when Fourier transforming back to p_\perp space, the integrand diverges along the path of integration due to the Landau pole at $1/b \sim \Lambda_{QCD}$. However looking at the form of the cross section, the integrand over b contains the Bessel function of first kind with argument bp_\perp and an exponent which contains powers of $\sim \log(M_h b)$. The combination of these two factors quickly damps out the integrand outside the region $1/p_\perp > b > 1/m_h$. Thus to avoid hitting the pole, we can simply put a sharp cut off for b at a value sufficiently higher than the largest value of $1/p_\perp \sim 0.5 \text{ GeV}^{-1}$ but smaller than $1/\Lambda_{QCD}$. A convenient value is found to be $b \sim 2 \text{ GeV}^{-1}$. It has been numerically ascertained that the variation of this cut-off between the values of $1.5 - 3 \text{ GeV}^{-1}$ produces an error only in the fourth significant digit of the integral.

5 The Fixed Order Cross Section and Power Corrections

When we match the full theory onto SCET we drop terms which are beyond leading order in $\lambda = p_\perp/M_h$. However, a comparison of the full theory fixed order cross section([10]) with the effective theory calculation reveals that in order to achieve ten percent accuracy, we need to include these higher order terms in λ beyond $p_\perp > 30 \text{ GeV}$. In principle we could achieve this by keeping higher order terms in the factorization theorem. However, this would only be necessary if we wished to resum the logs associated with these power corrections. Given that these power corrections are only relevant in regions of larger p_\perp , these logs are not numerically large and thus represent a small corrections which need not be resummed. At large p_\perp we

should turn off the resummation and use the fixed order NNLO result. Thus we subtract out the logs from the NNLO correction so that we do not double count, and turn off the resummation using scale profiles which we now consider.

6 Profiles

The SCET formalism we have used retains the leading order operators in the power counting parameter λ . This restricts the validity of the resummed cross-section to the regime where $p_\perp \ll M_h$. At larger values of p_\perp/M_h the resummation becomes superfluous. Moreover, the power corrections from subleading operators become increasingly relevant and to maintain accuracy it is vital to include these power corrections, as discussed above. So it is desirable to smoothly switch over from the resummed result to the full theory fixed order cross section when the singular and non-singular terms of the cross-section are comparable. Notice that formally, it is not necessary to turn off the resummation. As long as one makes the proper subtraction to avoid double counting, then the resummed terms that are kept should be sub-leading in the logarithmic power counting, since we are in the transition region. However, as discussed in the introduction, the fixed order result involves the cancellation between singular and non singular terms. If the scale of the log is not chosen appropriately (of order p_\perp) then this cancellation is not effective and the cross section is over estimated beyond the canonical scale variation errors⁶. This will be demonstrated below.

The shutting down of the resummation is achieved by varying the low matching scale from its value $1/b_0$ in the low p_\perp region to M_h in the high p_\perp region. This has the effect of turning off the resummed exponent. To do this, we introduce profiles in μ, ν following the work done in [7, 8]. We use three typical profiles for varying the renormalization scale from $1/b_0$ to M_h . Each profile is chosen as a linear combination of hyperbolic tangent functions which smoothly transitions from the resummation region to the fixed order one. The general equation for each profile P can be written as

$$P(s, L, H, P, t) = \frac{L}{2} \left(1 - \tanh \left[s \left(\frac{4P}{t} - 4 \right) \right] \right) + \frac{H}{2} \left(1 + \tanh \left[s \left(\frac{4P}{t} - 4 \right) \right] \right), \quad (6.1)$$

where s determines the rate of transition, $L = 2e^{-\gamma_E}/b$ is the initial value and $H = M_h$ is the final value. t is the value about which the transition is centered. Fig. (2) shows three profiles with $s = 2$ and $t = (35, 45, 55) \text{ GeV}$.

7 Error analysis

In our formalism, we have performed an expansion of the cross-section in M_h/m_t , p_\perp/M_h , Λ_{QCD}/p_\perp and the strong coupling α_s . Therefore, the dominant error in our cross-section is due to the first sub-leading term that we drop in each of these parameters. When expanding

⁶We thank Iain Stewart for discussions on this point.

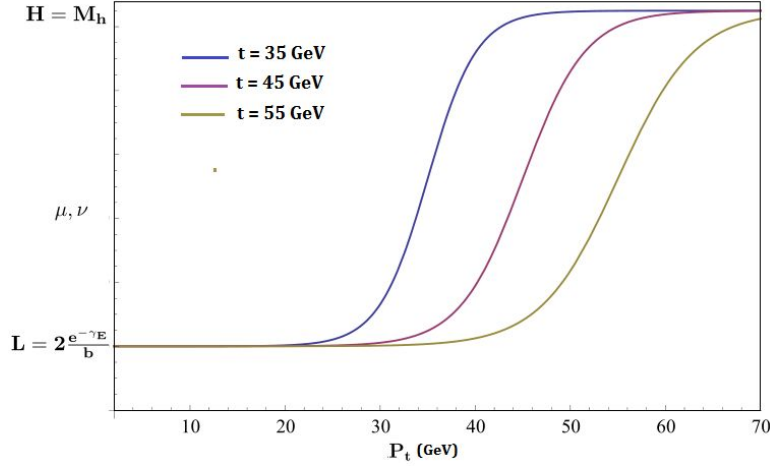


Figure 2. Profiles for turning off resummation

in M_h/m_t , we retain only the leading order operator. A comparison of the cross section in this limit with the exact m_t dependent result [10, 11], reveals that this approximation works extremely well for $p_\perp < m_t$. For the range of p_\perp discussed in this paper, the error due to these corrections is less than 1 %. For the parameter p_\perp/M_h , again we retain only the leading order operator. This approximation works well for $p_\perp \leq 30$ GeV as the leading correction scales as p_\perp^2/M_h^2 . As discussed earlier, for larger values of p_\perp , we include the full NNLO expression which includes all orders in p_\perp/M_h .

For the third parameter, Λ_{QCD}/p_\perp one must consider the non-perturbative contributions. Unlike the case of a central veto [44] there is more than one relevant non-perturbative parameter. The reason is that we are working in SCETII where the collinear and soft function both have the same invariant mass scale. As such, there will be non-perturbative contributions coming from both of these sectors. As p_\perp approaches Λ_{QCD} , we need to systematically include higher dimensional operators in both the soft and the beam sectors. There are multiple non-perturbative functions which contribute in this regime. In principle these matrix elements can be fit to the data. Work in this direction has been performed for vector boson production where ansatzes [47] for these matrix elements have been fit to the data [45]. However, since we are interested in a gluon initiated process we can not hope to use any extraction from the quark initiated vector boson production process. Therefore we make no attempt to model these corrections and simply include a rough estimate of the errors due to these terms by assuming an error which scales as $\Lambda_{QCD}^2/p_\perp^2$.

Finally we consider the errors due to higher order perturbative corrections. The accepted methodology for estimation of these errors is to vary the scale μ by factors of two. The idea is that such variations estimate the size of the constant terms which are not captured by the renormalization group, as well as the sensitivity to the perturbative truncation of the

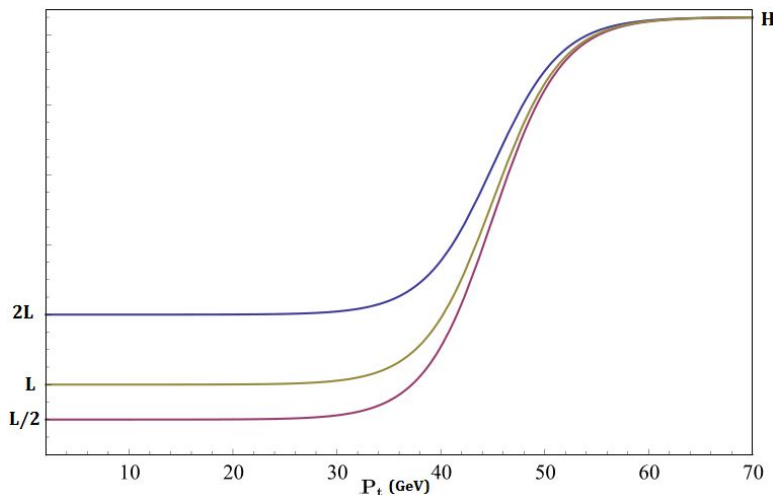


Figure 3. low p_T scale variation

anomalous dimensions. Of course this is just a rough guess which falls into the rubric of “you do the best you can,” though it is important to try to gauge all sources of large logarithms in these variations.

When working with the RRG we generalize this technique since we now have two distinct types of factorizations, virtuality and rapidity, and within the RRG there are therefore two distinct exponentiations. In both cases there is a choice as to what sub-leading terms should go into the exponent. Varying the scales μ, ν corresponds to varying the size of these sub-leading pieces. Given that virtuality and rapidity factorization are independent mechanisms we should vary both of these scales in order to estimate the errors in the choice of exponents.

This variation is accomplished by adjusting the parameter L in each profile which sets the scale for the low scale matching of the jet and soft function that dominates the perturbative errors. In keeping with the canonical recipe adopted by the community we vary L by a factor of two about its central value ($1/b_0$). The corresponding modification in the profiles for either μ or ν is shown in the Fig.3. When we vary these scales we must keep in mind the restriction that the argument of each large log is varied at most by a factor of two. This gives us a constraint $0.5 \leq \mu/\nu \leq 2$ since there are logs of the form $\ln(\mu/\nu)$ in the exponent. In all, this provides us with six different possibilities for each of the three profiles (Fig. 2). We do a similar analysis for the end point region of each profile by varying the scale H (Fig.4). Since this region of transverse momentum is dominated by the fixed order cross section, the variation in H amounts to a fixed order scale variation. We choose to keep the largest error band generated due to these variations. The plots which combine all the effects above, are shown in Fig.5 and Fig.6 for $S = 8$ and 14 TeV. We use the MSTW 2008 pdf at NNLO [51] and the value $\alpha_s(M_z) = 0.1184$.

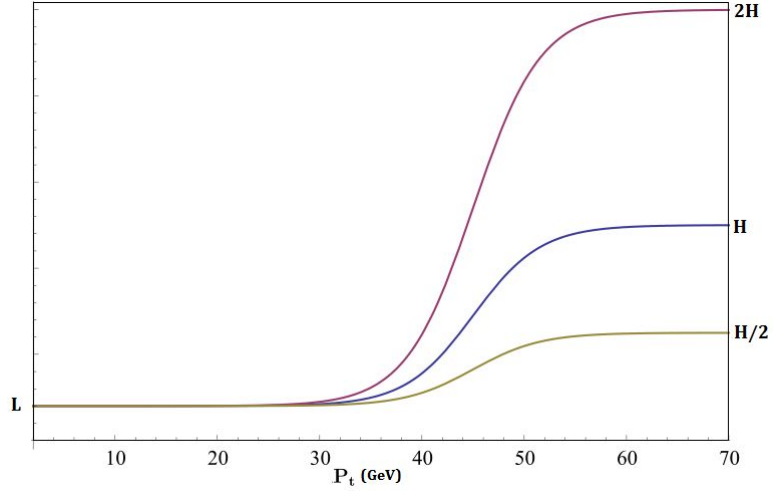


Figure 4. High p_T scale variation

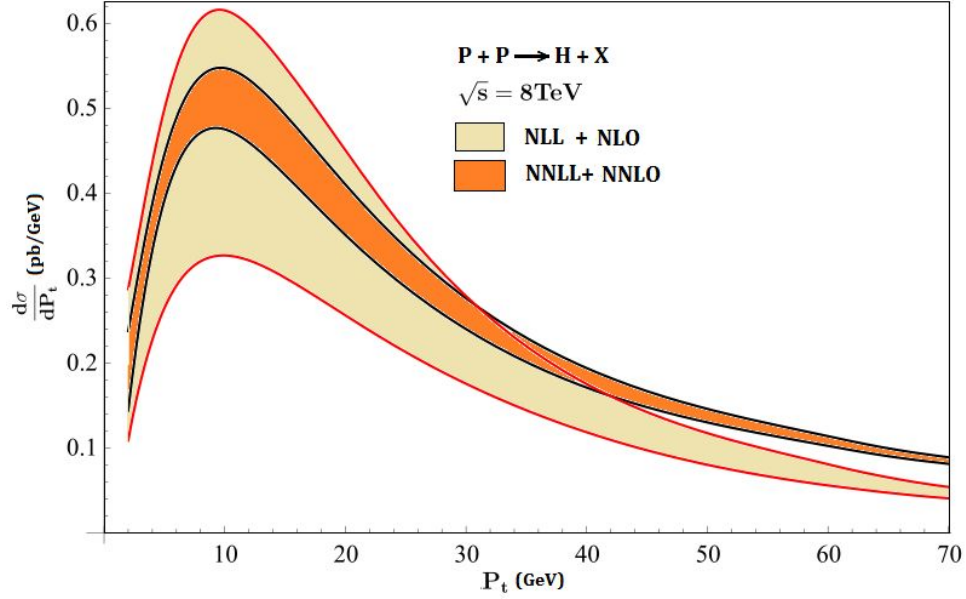


Figure 5. Cross section at 8 TeV

We also consider how the cross section is typically affected by using other pdf sets. In particular we evaluate the cross section at 13 TeV with the CTEQ5 pdf. The deviation from the MSTW2008 result is of the order of a few percent as shown in Fig.7. We include these errors as well in the final plot for the cross section at 13 TeV Fig.8.

8 Comparison to Previous Results

Let us now compare our results with the previous results in the literature which include the $NNLL$ resummation. We will compare only with those papers which show plots which include all of the corrections considered here, i.e. [21, 52]. We agree formally with the results of these papers. Of course formal agreement is not necessarily the relevant issue. Formal agreement means that the coefficients of the logs in the resummed result (as well as the non-singular pieces) agree. However, it does not mean that the argument of the logs are the same. Indeed for sufficiently different arguments the results can differ by an amount which is well outside any “reasonable” theoretical error estimation.

In the work [21] the authors calculate the spectrum up to 60 GeV and match onto the NLO result. Terms of order α^2 are not included which is consistent as long as one presumes that $\frac{\alpha}{\pi}\ln(60^2/mh^2) \sim 1$. That is, as long as the logs still dominate all the way up to $p_\perp = 60\text{ GeV}$, then keeping the terms of order α^2 would not improve the accuracy of the calculation. The results in [21] don't track the rapidity scale. Meaning that an implicit fixed matching scale has been chosen. In contrast to [21], the NNLL error band in our analysis lies within the error band of NLL. The reason is mainly two fold. They have no rapidity scale to vary and they have no errors due to non-perturbative corrections. This elucidates the importance of including the scale ν in error analysis for a better estimation of accuracy at each order in resummation. Further, the authors claim the existence of a non-perturbatively generated hard scale on the order of 8 GeV , which they state cuts off the non-perturbative corrections

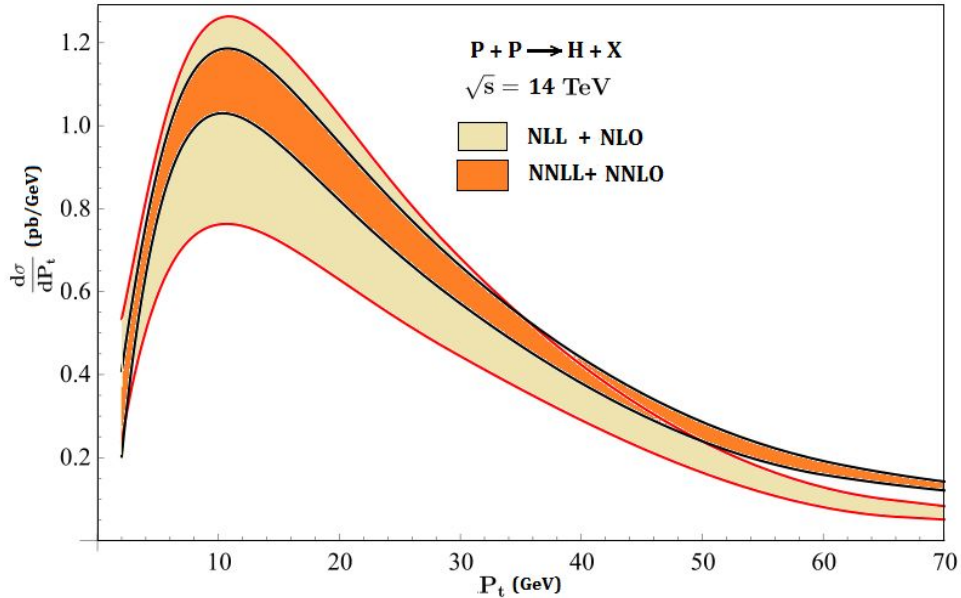


Figure 6. Cross section at 14 TeV

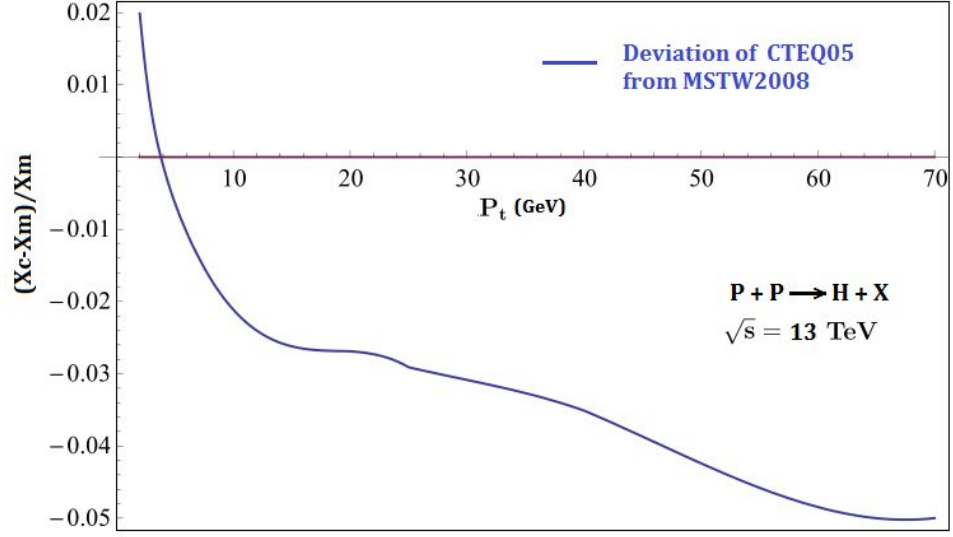


Figure 7. Comparison between pdf sets MSTW2008 and CTEQ05. The y axis plots the fraction of the difference between the central values of the cross section using the two sets

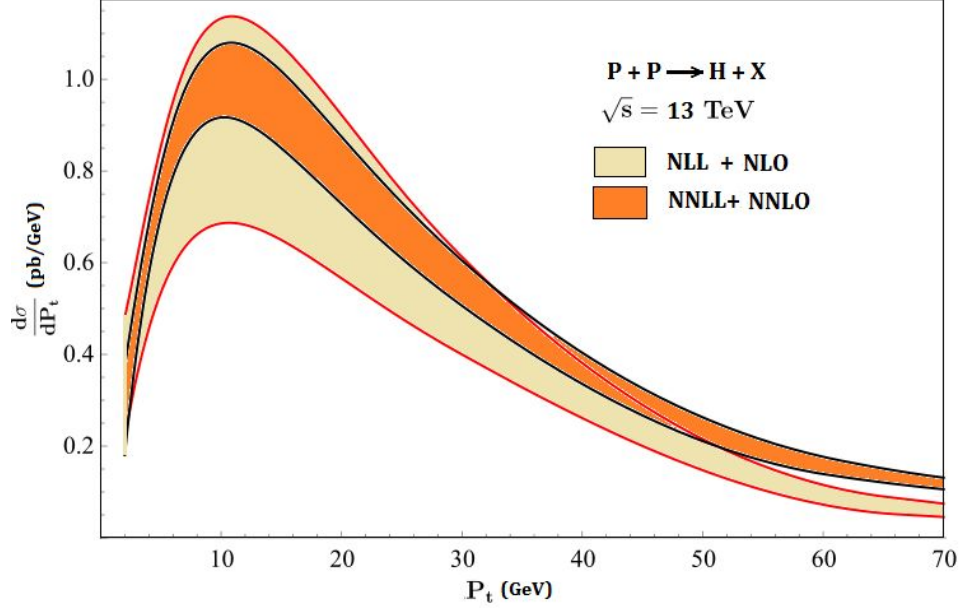


Figure 8. Cross section at 13 TeV

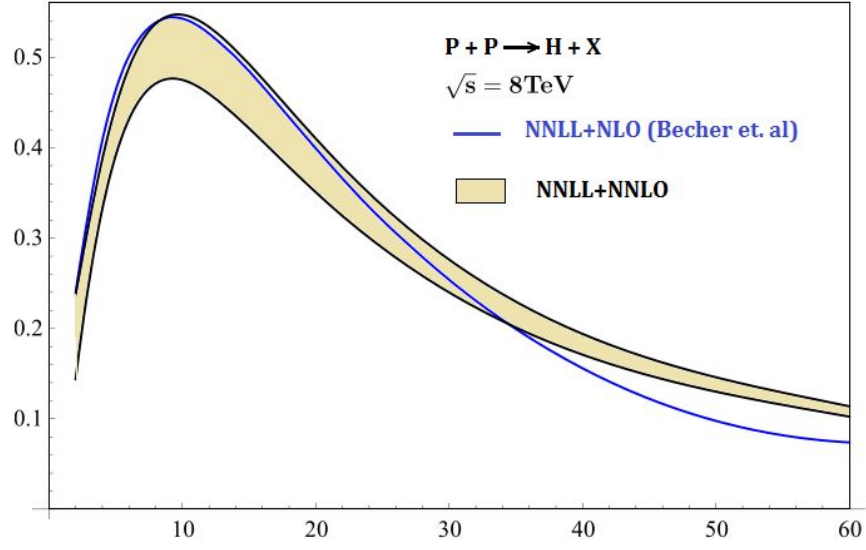


Figure 9. Comparison with Becher et. al.

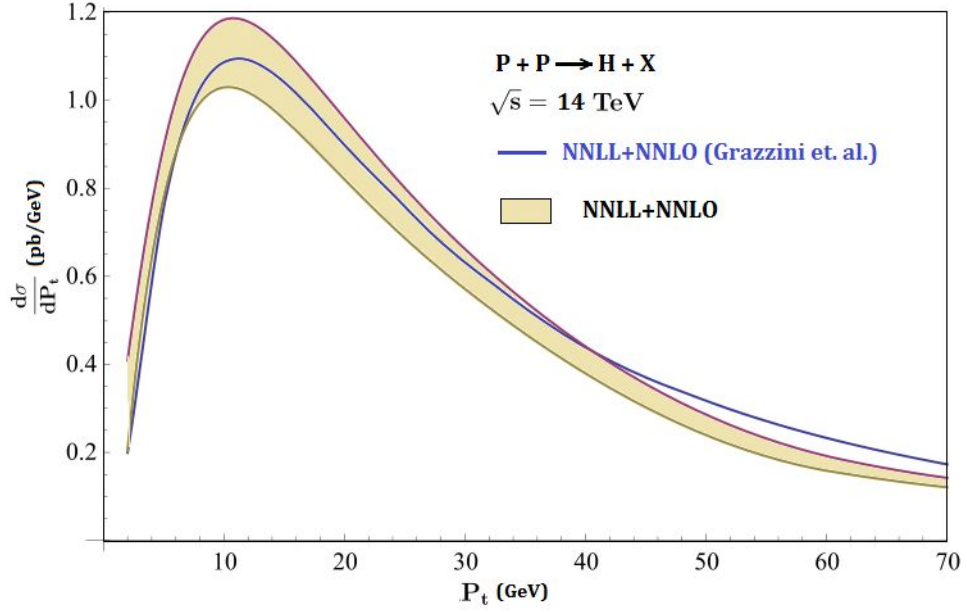


Figure 10. Comparison with CSS formalism

and therefore there results are valid down to vanishing p_\perp . The underlying justification is based on the paper [50] where it was argued that since in QED the probability to emit a photon with $p_\perp \sim 0$ vanishes faster than any value of Q^2 , the only contribution to the rate must come from two photons whose total p_\perp approximately vanishes but whose individual p_\perp is large. The authors of [50] then conjecture that the same reasoning should hold in the non-Abelian case. A recent study of the non-perturbative contributions to the TMDPDF can be found in [55] and we invite the reader to consult this paper for further information on the validity of these claims. Fig. 9 shows a comparison with their central value at NNLL+NLO. For larger values of p_\perp , the central value curve is below our estimates since the matching is done with fixed order NLO.

Grazzini et. al. [52] use the CSS formalism and plot the result out to 120 GeV, matching onto the fixed order result at NNLO. They do include an additional scale they call the resummation scale Q , in addition to the factorization scale of the PDFs and the renormalization scale of α . The variation of Q variation mixes what we would call μ and ν radiation. This is discussed in detail in the appendix. To turn off the resummation in the exponent they make the replacement

$$\text{Log}(Q^2 b^2/b_0) \rightarrow \text{Log}(Q^2 b^2/b_0 + 1) \quad (8.1)$$

this has the effect of killing the resummation at asymptotically small b and insuring that the total inclusive cross section is reproduced. However, in the range $M_h/p_\perp \sim 1$ the resummation is not shut off rapidly enough. Indeed, our results disagree with [52] for the central values by an amount which is larger than the theory error bars in the tail region as can be seen in Fig. 10. The reasons for this overshoot, as discussed above, is that if one does not use a profile to shut off the resummation beyond the transition region, then the scale of the log in the large p_\perp region is such that the singular and non-singular terms in the fixed order cross section no longer cancel as they do in the fixed order result. This effect is a recurring theme in the literature [44, 48, 49]. The authors of [52] also include the two loop matching to the hard function and show that its effects are at the one percent level. Moreover, without the other pieces of the calculation of this order, 4-loop cusp, 3 loop non-cusp, two loop soft and collinear matching, this inclusion does not increase the accuracy of the calculation. Regarding the scale variation, the authors vary three distinct scales as was performed in this paper. The variations mix rapidity and renormalization group scale dependence (see appendix) and one could argue that this is perhaps not as clean as varying μ and ν independently. But given that the scale variation technique is a blunt instrument to estimate perturbative uncertainty, it is not clear that distinguishing logs is quantitatively relevant, as long as all resummed logs are probed in the variation. The uncertainty bands in [52] are very close to those presented here. In the appendix we show how the work of Grazzini et. al. can be parsed in terms of the RRG.

Finally, a recent paper [54] working within the TMDPDF formalism of [24, 25, 27] published a cross-section for the Higgs transverse momentum distribution at NNLL, with no fixed order matching. The error bands are very small, with no overlap between the NLL and the

NNLL resummation, which the authors noted as a sign that they had under-estimated the perturbative uncertainty. The bands were generated by varying the resummation scales generated by the μ evolution of the TMDPDFs, after the resummation of the rapidity logs, which followed the procedure of [56]. The rapidity resummation scales were taken as fixed quantities. Thus no attempt was made to directly gauge the *perturbative* uncertainty in the rapidity resummation, that is, the perturbative uncertainty in the Collins-Soper kernel, whose exponentiation also resums the rapidity logarithms. Interestingly, variation of the non-perturbative models for the Collins-Soper kernel produced a much larger impact on the cross-section, see Fig. 4 of [54]. Since these non-perturbative models are explicitly exponentiated with the perturbative Collins-Soper kernel, in our view, this variation of the non-perturbative model parameters then may not be an estimate of the non-perturbative physics at all, but a more indirect gauge of the perturbative truncation of the Collins-Soper kernel and the rapidity resummation. Separating out the effects of the perturbative uncertainty in the Collins-Soper kernel, which has not been studied in the literature, will prove important in isolating the non-perturbative physics of the TMDPDFs.

9 Conclusion

The next LHC runs promises to shed more light on the nature of the Higgs boson. Here we have attempted to give the most accurate result possible for the transverse Higgs spectrum using the currently available theoretical calculations for matching coefficients, anomalous dimensions as well as the fixed order cross section. We resum the large logs in the low p_\perp region to NNLL and match this result to the fixed order cross section for high values of transverse momentum. To maintain accuracy over the complete range of the transverse momentum, we have utilized profiles in both the virtuality (μ) and rapidity (ν) factorization scales which smoothly turns off the resummation and matches onto the NNLO fixed order cross section at large values of p_\perp . This procedure prevents the problem of enhancing the fixed order result. We discuss the sources of error and ways to effectively estimate them using possible variations in the rapidity and renormalization scales for the profiles introduced. While we get a good agreement with previous results in the low p_\perp region, we get a lower estimate for the cross section in the transition and tail region.

The code which generated the plots in this paper is available upon request.

10 Acknowledgements

This work is supported by DOE contracts DOE-ER-40682-143 and DEACO2-C6H03000. D.N. is also supported by a MIT Pappalardo fellowship, and DOE contracts DE-SC00012567 and DE-SC0011090. D.N. also wishes to thank Simone Marzani for discussions of the literature.

A RRG resummation

In this appendix, we review the RRG formalism for the purpose of explicitly comparing to the method used in [31, 32, 53]. After integrating over the rapidity of the Higgs, the differential cross section is given by

$$\frac{d\sigma}{dp_t^2} = \sigma_0 \int \frac{dx_1}{x_1} \frac{dx_2}{x_2} \int d^2\vec{b} e^{i\vec{b} \cdot \vec{p}_t} \delta(m_h - Sx_1x_2) H(m_h, \mu) f_{n\perp}(x_1, \vec{b}, \mu, \nu) f_{\bar{n}\perp}(x_2, b, \mu, \nu) S(\vec{b}, \mu, \nu), \quad (\text{A.1})$$

where we have written out the explicit momentum fraction dependence. Since we are focusing on the resummation, we will often suppress the other arguments of the renormalized functions. The soft and beam functions have the μ -anomalous dimension:

$$\mu \frac{d}{d\mu} \ln S(\nu, \mu) = \Gamma_R[\alpha_s(\mu)] \ln\left[\frac{\mu}{\nu}\right] + \gamma_s(\alpha_s(\mu)), \quad (\text{A.2})$$

$$\mu \frac{d}{d\mu} \ln f_{\perp}(\nu, \mu) = \frac{1}{2} \Gamma_R[\alpha_s(\mu)] \ln\left[\frac{\nu}{m_h}\right] + \gamma_{f\perp}(\alpha_s(\mu)). \quad (\text{A.3})$$

Using the fact that the RG and RRG variations of the amplitude must commute, we can write the rapidity anomalous dimension as integral over the μ anomalous dimensions [14, 15] and a constant piece

$$\nu \frac{d}{d\nu} \ln S(\nu, \mu) = \int_{(\frac{be^{\gamma_E}}{2})^{-1}}^{\mu} \frac{dq}{q} \Gamma_R[\alpha_s(q)] + \gamma_R\left[\alpha_s\left(\left(\frac{be^{\gamma_E}}{2}\right)^{-1}\right)\right], \quad (\text{A.4})$$

$$\nu \frac{d}{d\nu} \ln f_{\perp}(\nu, \mu) = -\frac{1}{2} \int_{(\frac{be^{\gamma_E}}{2})^{-1}}^{\mu} \frac{dq}{q} \Gamma_R[\alpha_s(q)] - \frac{1}{2} \gamma_R\left[\alpha_s\left(\left(\frac{be^{\gamma_E}}{2}\right)^{-1}\right)\right]. \quad (\text{A.5})$$

Writing things in this way allows for there to be large μ dependent logs which may arise depending upon the choice of μ . As noted in Sec. 4, Γ_R is related to the cusp anomalous dimension. The non-cusp piece of the rapidity anomalous dimension $\gamma_R\left[\alpha_s\left(\left(\frac{be^{\gamma_E}}{2}\right)^{-1}\right)\right]$ can be extracted from the calculation of the soft function at the renormalization point $\mu = \left(\frac{be^{\gamma_E}}{2}\right)^{-1}$. This is a choice of scheme which defines the scale in the Log which multiplies the cusp anomalous dimension.

We run the beam/soft functions in ν from ν_s and m_h to ν respectively

$$S(\vec{b}, \mu, \nu) = U_S^{RRG}\left(\vec{b}, \mu, \frac{\nu}{\nu_s}\right) S(\vec{b}, \mu, \nu_s), \quad (\text{A.6})$$

$$f_{n\perp}(x, \vec{b}, \mu, \nu) = U_F^{RRG}\left(\vec{b}, \mu, \frac{\nu}{m_h}\right) f_{n\perp}(x, \vec{b}, \mu, m_h). \quad (\text{A.7})$$

Note that we have explicitly chosen $\nu_B = m_h$ in the TMDPDF. The full RRG factor has the rapidity factorization scale ν cancel in the exponent, and gives:

$$U_{SF^2}^{RRG}\left(\vec{b}, \mu, \frac{m_h}{\nu_s}\right) = \text{Exp}\left[\ln\left(\frac{m_h}{\nu_s}\right) \left\{ \int_{(\frac{be^{\gamma_E}}{2})^{-1}}^{\mu} \frac{dq}{q} \Gamma_R[\alpha_s(q)] + \gamma_R\left[\alpha_s\left(\left(\frac{be^{\gamma_E}}{2}\right)^{-1}\right)\right] \right\}\right]. \quad (\text{A.8})$$

We also need the μ evolution of the TMDPDFs at $\nu = m_h$ and the soft function at $\nu = \nu_s$. With these scale choices, the TMDPDF has no double log- μ evolution, so one obtains:

$$f_{\perp}(x, \vec{b}, \mu, \nu = m_h) = \text{Exp} \left[\int_{\mu_i}^{\mu} \frac{dq}{q} \gamma_{f_{\perp}}[\alpha_s(q)] \right] f_{\perp}(x, \vec{b}, \mu_i, \nu = m_h),$$

$$S(\vec{b}, \mu, \nu = \nu_s) = \text{Exp} \left[\int_{\mu_i}^{\mu} \frac{dq}{q} \left\{ \ln\left(\frac{\nu_s}{q}\right) \Gamma_R[\alpha_s(q)] + \gamma_s[\alpha_s(q)] \right\} \right] S(\vec{b}, \mu_i, \nu = \nu_s). \quad (\text{A.9})$$

Combining these pieces together, we achieve the full resummation kernel for the cross-section:

$$f_{n\perp}(\mu, \nu) f_{\bar{n}\perp}(\mu, \nu) S(\mu, \nu) = R(\mu, \mu_i, \nu_s, m_h, b) f_{n\perp}(\mu_i, m_h) f_{\bar{n}\perp}(\mu_i, m_h) S(\mu_i, \nu_s) \quad (\text{A.10})$$

$$R(\mu, \mu_i, \nu_s, m_h, b) = \text{Exp} \left[\int_{\mu_i}^{\mu} \frac{dq}{q} \left\{ \ln\left[\frac{m_h}{q}\right] \Gamma_R[\alpha_s(q)] + \gamma_s[\alpha_s(q)] + 2\gamma_{f_{\perp}}[\alpha_s(q)] \right\} \right. \\ \left. + \ln\left[\frac{m_h}{\nu_s}\right] \left\{ \int_{\left(\frac{be^{\gamma_E}}{2}\right)^{-1}}^{\mu_i} \frac{dq}{q} \Gamma_R[\alpha_s(q)] + \gamma_R\left[\alpha_s\left(\left(\frac{be^{\gamma_E}}{2}\right)^{-1}\right)\right] \right\} \right] \quad (\text{A.11})$$

From the form of (A.11), we can directly see the variation of the independent resummation scales μ, μ_i, ν_s probe different exponentiated logs, thus giving estimates of the subleading terms in the perturbative expansions. The double logarithmic terms associated with μ_i cancel manifestly in the exponent⁷, and thus the μ_i variation is estimating the subleading terms associated with $\gamma_{s, f_{\perp}}$. We can eliminate large logs of the impact parameter from the beam and soft function matrix elements by choosing the scales μ_i, ν_s appropriately. Four potential schemes for canonical scale choices are:

- A : $\mu_i = \nu_s = \left(\frac{be^{\gamma_E}}{2}\right)^{-1}$
- B : $\mu_i = p_T, \nu_s = \left(\frac{be^{\gamma_E}}{2}\right)^{-1}$
- C : $\mu_i = \left(\frac{be^{\gamma_E}}{2}\right)^{-1}, \nu_s = p_T$
- D : $\mu_i = \nu_s = p_T$

As noted in [57], making scale choices in either momentum space or conjugate space can have a sizable numerical impact on the cross-section, as well as how accurately the resummation captures the higher order logs claimed by the resummation. Scale setting in momentum space, residual logs can exist in the plus distributions of the low scale theory that become apparent only after integrating the resummation kernel against the matrix elements, in this case, the

⁷Though depending on how one handles the integration over the running coupling, this cancellation could be incomplete. An incomplete cancellation could be used to give another handle on estimating the uncertainty in the double logarithmic terms.

TMDPDF and the soft function. Scale setting in conjugate space does not suffer from this ambiguity. Specifically, for the canonical choice $\nu_s = \mu_i = (\frac{be^{\gamma_E}}{2})^{-1}$, R becomes:

$$R(\mu, m_h, b) = \text{Exp} \left[\int_{(\frac{be^{\gamma_E}}{2})^{-1}}^{\mu} \frac{dq}{q} \left\{ \ln \left[\frac{m_h}{q} \right] \Gamma_R[\alpha_s(q)] + \gamma_s[\alpha_s(q)] + 2\gamma_{f\perp}[\alpha_s(q)] \right\} \right. \\ \left. + \ln \left[m_h b e^{\gamma_E} \right] \gamma_R[\alpha_s((\frac{be^{\gamma_E}}{2})^{-1})] \right]. \quad (\text{A.12})$$

A.1 Comparision to Grazzini et al.

We now write out the resummation formalism used in [52], as derived in [31, 32, 53], suppressing the flavor sum in the PDFs:

$$\frac{d\sigma}{dp_t^2} = \int \frac{dx_1}{x_1} \frac{dx_2}{x_2} \int \frac{d^2\vec{b}}{4\pi} e^{i\vec{b}\cdot\vec{p}_t} f(x_1, \mu_F) f(x_2, \mu_F) \mathcal{W} \left(b, m_h, x_1 x_2, \mu_R, \mu_F \right) \quad (\text{A.13})$$

Then one switches to moment space by integrating $\frac{1}{z} = x_1 x_2$ for \mathcal{W} :

$$\mathcal{W}_N \left(b, m_h, \mu_R, \mu_F \right) = \int_0^1 dz z^{N-1} \mathcal{W} \left(b, m_h, \frac{1}{z}, \mu_R, \mu_F \right) \quad (\text{A.14})$$

The authors write this as

$$\mathcal{W}_N \left(b, m_h, \mu_R, \mu_F \right) = \mathcal{H}_N \left(m_h, \mu_R, \mu_F; Q \right) \text{Exp} \left[\mathcal{G}_N \left(b, m_h, \mu_R, Q \right) \right]. \quad (\text{A.15})$$

Note that the factorization scale from the PDFs is in the function \mathcal{H} . Then the form of the resummed exponent is:

$$\mathcal{G}_N \left(b, m_h, \mu_R, Q \right) = - \int_{b^2 e^{2\gamma_E}}^{Q^2} \frac{dq^2}{q^2} \left\{ A[\alpha_s(q)] \ln \left(\frac{m_h^2}{q^2} \right) + B_N[\alpha_s(q)] \right\} \quad (\text{A.16})$$

Note that B_N has PDF running in it since it depends on the moment N . The function \mathcal{H}_N is claimed to have no large logarithms, and can be perturbatively calculated. To one loop:

$$\mathcal{H}_N \left(m_H, \mu_R, \mu_F; Q \right) = 1 + \frac{\alpha_s}{\pi} \left(H^{(1)} + 2C_N^{(1)} - p\beta_0\ell_R + 2\gamma_N\ell_F - (\frac{1}{2}A^{(1)}\ell_Q + B^{(1)} + 2\gamma_N^{(1)}\ell_Q) \right) \quad (\text{A.17})$$

Where:

$$\ell_R = \ln \frac{m_h^2}{\mu_R^2} \quad \ell_F = \ln \frac{m_h^2}{\mu_F^2} \quad \ell_Q = \ln \frac{m_h^2}{Q^2} \quad (\text{A.18})$$

And:

$$A^{(1)} = C_A \quad (\text{A.19})$$

$$B^{(1)} = -\frac{1}{6}(11C_A - 2N_f) \quad (\text{A.20})$$

$$\gamma_N^{(1)} = \int_0^1 dz z^{N-1} P^{(1)}(z) \quad (\text{A.21})$$

C_N is related to the order ϵ pieces of the DGLAP splitting kernels. $H^{(1)}$ is the hard matching, but also contain terms in the $\delta(1-z)$ pieces of the TMDPDF. Note that $\mu_R \sim \mu_F \sim Q \sim m_h$, so that the PDFs are run from Λ_{QCD} to the high scale, implicitly.

By choosing the appropriate scales, we can connect the resummed formula of (A.16) to the resummation formulas of (A.11) and (A.12). We must also apply the resummation scale prescription of [53], where all large logs are split:

$$\ln[m_h(\frac{be^{\gamma_E}}{2})^{-1}] \rightarrow \ln\left[\frac{m_h}{Q}\right] + \ln\left[Q(\frac{be^{\gamma_E}}{2})^{-1}\right] \quad (\text{A.22})$$

and any log of $\ln\left[\frac{m_h}{Q}\right]$ is expanded out of the exponent and included in the hard function of (A.15). Setting $\mu = Q$ in (A.12), this gives:

$$R(Q, m_h, b) = \text{Exp} \left[\int_{(\frac{be^{\gamma_E}}{2})^{-1}}^Q \frac{dq}{q} \left\{ \ln\left[\frac{m_h}{q}\right] \Gamma_R[\alpha_s(q)] + \gamma_s[\alpha_s(q)] + 2\gamma_{f\perp}[\alpha_s(q)] + \gamma_R[\alpha_s((\frac{be^{\gamma_E}}{2})^{-1})] \right\} \right. \\ \left. + \ln\left[\frac{m_h}{Q}\right] \gamma_R[\alpha_s((\frac{be^{\gamma_E}}{2})^{-1})] \right], \quad (\text{A.23})$$

choosing $Q = \mu$ this result is identical to (A.12).

The hard function of Eq. (A.15) is explicitly given to two loops in [53], and one can verify the factor $\ln\left[\frac{m_h}{Q}\right] \gamma_R[\alpha_s((\frac{be^{\gamma_E}}{2})^{-1})]$ in (A.23) is expanded out of the exponent and then included in the $B^{(2)}$ term of the hard matching. Indeed, from the form of the hard function given in [53], one can see the resummation scale Q probes both rapidity logs and RG logs since $B^{(2)}$ includes both types of anomalous dimensions. This explains the similar sized perturbative error estimation of this paper, and that of [52].

References

- [1] CERN Report No. ATLAS-CONF-029 (unpublished).
CERN Report No. ATLAS-CONF-031 (unpublished).
CMS Collaboration, CMS-PAS-HIG-13-003 (unpublished).
- [2] U. Langenegger, M. Spira, A. Starodumov and P. Trueb, JHEP **0606**, 035 (2006) [hep-ph/0604156], C. Arnesen, I. Z. Rothstein and J. Zupan, Phys. Rev. Lett. **103**, 151801 (2009) [arXiv:0809.1429 [hep-ph]], C. Grojean, E. Salvioni, M. Schlaffer and A. Weiler, JHEP **1405**, 022 (2014) [arXiv:1312.3317 [hep-ph], arXiv:1312.3317], M. Schlaffer, M. Spannowsky, M. Takeuchi, A. Weiler and C. Wymant, Eur. Phys. J. C **74**, no. 10, 3120 (2014) [arXiv:1405.4295 [hep-ph]], S. Dawson, I. M. Lewis and M. Zeng, arXiv:1501.04103 [hep-ph].

- [3] C. W. Bauer, S. Fleming, and M. E. Luke,, *Phys. Rev. D* **63** (2000) 014006, [hep-ph/0005275],
C. W. Bauer, S. Fleming, D. Pirjol, and I. W. Stewart, , *Phys. Rev. D* **63** (2001) 114020,
[hep-ph/0011336], C. W. Bauer, D. Pirjol, and I. W. Stewart, , *Phys. Rev. D* **65** (2002) 054022,
[hep-ph/0109045], C. W. Bauer, S. Fleming, D. Pirjol, I. Z. Rothstein and I. W. Stewart,
Phys. Rev. D **66**, 014017 (2002) [hep-ph/0202088].
- [4] T. Becher and M. Neubert, Factorization and NNLL Resummation for Higgs Production with a
Jet Veto, *JHEP* **1207**, 108 (2012) [arXiv:1205.3806 [hep-ph]].
- [5] T. Becher, M. Neubert and L. Rothen, Factorization and N^3LL_p +NNLO predictions for the
Higgs cross section with a jet veto, *JHEP* **1310**, 125 (2013) [arXiv:1307.0025 [hep-ph]].
- [6] A. Banfi, G. P. Salam and G. Zanderighi, NLL+NNLO predictions for jet-veto efficiencies in
Higgs-boson and Drell-Yan production, *JHEP* **1206**, 159 (2012) [arXiv:1203.5773 [hep-ph]].
- [7] F. J. Tackmann, J. R. Walsh and S. Zuberi, Resummation Properties of Jet Vetoes at the LHC,
Phys. Rev. D **86**, 053011 (2012) [arXiv:1206.4312 [hep-ph]].
- [8] I. W. Stewart, F. J. Tackmann, J. R. Walsh and S. Zuberi, Jet p_\perp Resummation in Higgs
Production at $NNLL' + NNLO$, *Phys. Rev. D* **89**, no. 5, 054001 (2014) [arXiv:1307.1808].
- [9] V. Ravindran, J. Smith and W. L. Van Neerven, *Nucl. Phys. B* **634**, 247 (2002)
[hep-ph/0201114].
- [10] C. J. Glosser and C. R. Schmidt, Next-to-leading corrections to the Higgs boson transverse
momentum spectrum in gluon fusion, *JHEP* **0212**, 016 (2002) [hep-ph/0209248].
- [11] U. Baur and E. W. N. Glover, *Nucl. Phys. B* **339**, 38 (1990), V. Del Duca, W. Kilgore,
C. Oleari, C. Schmidt and D. Zeppenfeld, *Phys. Rev. Lett.* **87**, 122001 (2001) [hep-ph/0105129],
V. Del Duca, W. Kilgore, C. Oleari, C. Schmidt and D. Zeppenfeld, *Nucl. Phys. B* **616**, 367
(2001) [hep-ph/0108030].
- [12] T. Inami, T. Kubota, and Y. Okada, Effective Gauge Theory And The Effect Of Heavy Quarks
In Higgs Boson Decays, *Z.Phys. C18* (1983) 69.
- [13] R. V. Harlander, *Phys. Lett. B* 492, 74 (2000) [arXiv:hep-ph/0007289].
- [14] J. Y. Chiu, A. Jain, D. Neill and I. Z. Rothstein, The Rapidity Renormalization Group, *Phys.*
Rev. Lett. **108**, 151601 (2012) [arXiv:1104.0881 [hep-ph]].
- [15] J. Y. Chiu, A. Jain, D. Neill and I. Z. Rothstein, A Formalism for the Systematic Treatment of
Rapidity Logarithms in Quantum Field Theory, *JHEP* **1205**, 084 (2012) [arXiv:1202.0814
[hep-ph]].
- [16] S. Dawson, Radiative corrections to Higgs boson production, *Nucl. Phys. B* **359**, 283 (1991).
- [17] S. Mantry and F. Petriello, Factorization and Resummation of Higgs Boson Differential
Distributions in Soft-Collinear Effective Theory, *Phys.Rev. D* 81 (2010) 093007,
[arXiv:0911.4135].
- [18] S. Mantry and F. Petriello, Transverse Momentum Distributions from Effective Field Theory
with Numerical Results, *Phys. Rev. D* **83**, 053007 (2011) [arXiv:1007.3773 [hep-ph]].
- [19] V. Ahrens, T. Becher, M. Neubert and L. L. Yang, Renormalization-Group Improved
Prediction for Higgs Production at Hadron Colliders, *Eur. Phys. J. C* **62**, 333 (2009)
[arXiv:0809.4283 [hep-ph]].

- [20] T. Becher and M. Neubert, Drell-Yan production at small q_T , transverse parton distributions and the collinear anomaly, *Eur. Phys. J. C* **71** (2011) 1665, [arXiv:1007.4005]
- [21] T. Becher, M. Neubert and D. Wilhelm, Higgs-Boson Production at Small Transverse Momentum, *JHEP* **1305**, 110 (2013) [arXiv:1212.2621 [hep-ph]].
- [22] Y. Gao, C. S. Li, and J. J. Liu, Transverse momentum resummation for Higgs production in soft-collinear effective theory, *Phys.Rev. D* **72** (2005) 114020, [hep-ph/0501229].
- [23] A. Idilbi, X.-d. Ji, and F. Yuan, Transverse momentum distribution through soft-gluon resummation in effective field theory, *Phys.Lett. B* **625** (2005) 253263, [hep-ph/0507196].
- [24] M. G. Echevarria, A. Idilbi and I. Scimemi, Factorization Theorem For Drell-Yan At Low q_T And Transverse Momentum Distributions On-The-Light-Cone, *JHEP* **1207**, 002 (2012) [arXiv:1111.4996 [hep-ph]].
- [25] M. G. Echevarria, A. Idilbi and I. Scimemi, Soft and Collinear Factorization and Transverse Momentum Dependent Parton Distribution Functions, *Phys. Lett. B* **726**, 795 (2013) [arXiv:1211.1947 [hep-ph]].
- [26] U. D'Alesio, M. G. Echevarria, S. Melis and I. Scimemi, Non-perturbative QCD effects in q_T spectra of Drell-Yan and Z-boson production, *JHEP* **1411**, 098 (2014) [arXiv:1407.3311 [hep-ph]].
- [27] M. G. Echevarria, A. Idilbi, A. Schfer and I. Scimemi, Model-Independent Evolution of Transverse Momentum Dependent Distribution Functions (TMDs) at NNLL, *Eur. Phys. J. C* **73**, no. 12, 2636 (2013) [arXiv:1208.1281 [hep-ph]].
- [28] J. C. Collins, D. E. Soper, and G. F. Sterman, Transverse Momentum Distribution in Drell-Yan Pair and W and Z Boson Production, *Nucl. Phys. B* **250** (1985) 199.
- [29] I. Hinchliffe and S. F. Novaes, Transverse-momentum distribution of higgs bosons at the superconducting super collider, *Phys. Rev. D* **38** (Dec, 1988) 34753480.
- [30] R. P. Kauffman, Higgs-boson pt in gluon fusion, *Phys. Rev. D* **44** (Sep, 1991) 14151425.
- [31] D. de Florian and M. Grazzini, Next-to-next-to-leading logarithmic corrections at small transverse momentum in hadronic collisions, *Phys. Rev. Lett.* **85** (2000) 46784681, [hep-ph/0008152]
- [32] D. de Florian and M. Grazzini, The structure of large logarithmic corrections at small transverse momentum in hadronic collisions, *Nucl. Phys. B* **616** (2001) 247285, [hep-ph/0108273].
- [33] S. Catani and M. Grazzini, QCD transverse-momentum resummation in gluon fusion processes, *Nucl. Phys. B* **845** (2011) 297323, [arXiv:1011.3918]
- [34] G. Sterman and M. Zeng, *JHEP* **1405**, 132 (2014) [arXiv:1312.5397 [hep-ph]].
- [35] M. Bonvini, S. Forte, G. Ridolfi and L. Rottoli, *JHEP* **1501**, 046 (2015) [arXiv:1409.0864 [hep-ph]].
- [36] R. V. Harlander and K. J. Ozeren, *JHEP* **0911**, 088 (2009) [arXiv:0909.3420 [hep-ph]].
- [37] I. A. Korchemskaya and G. P. Korchemsky, *Phys. Lett. B* **287**, 169 (1992).
- [38] G. Parisi, *Phys. Lett. B* **90**, 295 (1980). , G. F. Sterman, *Nucl. Phys. B* **281**, 310 (1987), L. Magnea and G. F. Sterman, *Phys. Rev. D* **42**, 4222 (1990).

- [39] L. Magnea and G. F. Sterman, Phys. Rev. D **42**, 4222 (1990).
- [40] V. Ahrens, T. Becher, M. Neubert and L. L. Yang, Phys. Rev. D **79**, 033013 (2009) [arXiv:0808.3008 [hep-ph]].
- [41] I. W. Stewart, F. J. Tackmann, J. R. Walsh and S. Zuberi, Phys. Rev. D **89**, no. 5, 054001 (2014) [arXiv:1307.1808].
- [42] A. Vogt, S. Moch and J. A. M. Vermaseren, Nucl. Phys. B **691**, 129 (2004) [hep-ph/0404111].
- [43] S. Moch, J. A. M. Vermaseren and A. Vogt, Phys. Lett. B **625**, 245 (2005) [hep-ph/0508055].
- [44] C. F. Berger, C. Marcantonini, I. W. Stewart, F. J. Tackmann and W. J. Waalewijn, Higgs Production with a Central Jet Veto at NNLL+NNLO, JHEP **1104**, 092 (2011) [arXiv:1012.4480 [hep-ph]].
- [45] G. A. Ladinsky and C. P. Yuan, Phys. Rev. D **50**, 4239 (1994) [hep-ph/9311341].
- [46] R. V. Harlander, T. Neumann, K. J. Ozeren and M. Wiesemann, JHEP **1208**, 139 (2012) [arXiv:1206.0157 [hep-ph]].
- [47] C. T. H. Davies, B. R. Webber and W. J. Stirling, Nucl. Phys. B **256**, 413 (1985).
- [48] Z. Ligeti, I. W. Stewart and F. J. Tackmann, Phys. Rev. D **78**, 114014 (2008) [arXiv:0807.1926 [hep-ph]].
- [49] R. Abbate, M. Fickinger, A. H. Hoang, V. Mateu and I. W. Stewart, Phys. Rev. D **83**, 074021 (2011) [arXiv:1006.3080 [hep-ph]].
- [50] G. Parisi and R. Petronzio, Nucl. Phys. B **154**, 427 (1979).
- [51] A. D. Martin, W. J. Stirling, R. S. Thorne and G. Watt, Eur. Phys. J. C **63**, 189 (2009) [arXiv:0901.0002 [hep-ph]].
- [52] D. de Florian, G. Ferrera, M. Grazzini and D. Tommasini, JHEP **1111**, 064 (2011) [arXiv:1109.2109 [hep-ph]].
- [53] G. Bozzi, S. Catani, D. de Florian and M. Grazzini, Nucl. Phys. B **737**, 73 (2006) [hep-ph/0508068].
- [54] M. G. Echevarria, T. Kasemets, P. J. Mulders and C. Pisano, arXiv:1502.05354 [hep-ph].
- [55] J. Collins and T. Rogers, arXiv:1412.3820 [hep-ph].
- [56] J. Collins, (Cambridge monographs on particle physics, nuclear physics and cosmology. 32)
- [57] L. G. Almeida, S. D. Ellis, C. Lee, G. Sterman, I. Sung and J. R. Walsh, JHEP **1404**, 174 (2014) [arXiv:1401.4460 [hep-ph]].